JOURNAL OF MATERIALS PROCESSING TECHNOLOGY 205 (2008) 190–202

journal homepage: www.elsevier.com/locate/jmatprotec

Modeling tool wear progression by using mixed effects modeling technique when end-milling AISI 4340 steel

Pinaki Chakraborty[a], *Shihab Asfour*[a,*], *Sohyung Cho*[a], *Arzu Onar*[b], *Matthew Lynn*[c]

[a] *Manufacturing Engineering Laboratory, Department of Industrial Engineering, University of Miami, P.O. Box 248294, Coral Gables, FL 33124, USA*
[b] *Department of Biostatistics, St. Jude Children's Research Hospital, 332 North Lauderdale Street, Mail Stop 768, Memphis, TN 38105, USA*
[c] *Center for Advanced Microscopy, Department of Chemistry, University of Miami, 1301 Memorial Drive, Room 315, Coral Gables, FL 33146, USA*

ARTICLE INFO

Article history:
Received 24 September 2007
Received in revised form
6 November 2007
Accepted 15 November 2007

Keywords:
Mixed effects model
End-milling
TiN–TiAlN
Semi-dry machining
Dry machining
EDX analysis

ABSTRACT

Semi-dry and dry machining is being adopted by the metal cutting industry worldwide to reduce the harmful effects of traditional metal cutting fluids and the cost associated with procurement, use, and disposal of these fluids. This research focuses on end-milling of AISI 4340 steel with multi-layer physical vapor deposition (PVD) coated carbide inserts under semi-dry and dry cutting conditions and proposes a mixed effects model for the analysis of the longitudinal data obtained from a designed experiment. This modeling approach considers unobserved heterogeneity during machining and proposes a tool wear progression model that has a higher power of detecting effects of significant factors than traditional regression models. One such source of variation is work piece hardness that was observed within and across test blocks. From the wear progression model developed, the lowest initial flank wear values are obtained at a cutting speed of 183 m/min, a feed rate of 0.10 mm/rev under semi-dry cutting conditions. A higher rate of wear progression and lower tool life was observed at the higher cutting speed level of 229 m/min. Cutting speed has the most significant effect on flank wear progression in this study. Depth of cut on the other hand did not show any significant effect on tool wear when compared to cutting speed, feed and cutting conditions. The wear mechanism of the insert was analyzed using electron dispersive X-ray (EDX) and environmental scanning electron microscope (ESEM) images. From this analysis, diffusion wear was confirmed under both semi-dry and dry machining conditions. It is expected that the proposed model can reduce the number of repetitions in tool wear modeling experiment for tool manufacturers leading to substantial cost savings.

1. Introduction

Turning and milling are two widely used machining processes in the metal cutting industry. Majority of tool wear models in the metal cutting literature have been developed for turning which is an orthogonal machining process, whereas tool wear models for milling are relatively few due to the complexity in the process modeling (Alauddin and El Baradie, 1997). At present, increasing coolant costs, maintenance, disposal costs and new emission standards set forth by NIOSH,

* *Corresponding author*. Tel.: +1 305 607 7676; fax: +1 305 284 4040.
E-mail address: sasfour@miami.edu (S. Asfour).
0924-0136/$ – see front matter © 2007 Elsevier B.V. All rights reserved.
doi:10.1016/j.jmatprotec.2007.11.197

OSHA and ISO14001 are making dry and semi-dry machining increasingly attractive to the metal cutting industry in the United States and worldwide (What you need to know about occupational exposure to metal working fluids, 1998; Metalworking Fluids, Safety and Health Best Practices Manual, 1999; Autret and Liang, 2003). However, the research literature on tool wear models particularly for milling under dry and semi-dry machining conditions is sparse. Alauddin et al. (1995) studied tool wear progression for end-milling of hot forged and annealed Inconel 718 alloy using carbide inserts under dry machining conditions. In their study, full and half immersion up and down milling were used for experiments and arithmetic mean value of flank wear was plotted against machining time. Tool life was determined by cutting time in minutes taken by the insert to reach a threshold value, which was 0.75 mm of average non-uniform wear or localized flank wear. They observed variations in flank wear progression over time when the experiment was repeated under identical cutting conditions. Alauddin and El Baradie (1997) developed tool life models for slot end-milling of AISI 1020 cold rolled steel with uncoated cobalt alloyed high speed steel inserts under dry cutting conditions. They developed a first order and second order regression model for tool life prediction with different set of processing parameters for cutting speed, feed and depth of cut (DOC).

Dos Santos et al. (1999) used the extended Taylor tool life equation to predict tool life for face milling AISI 1045 cold rolled steel and AISI 304 stainless steel with triple TiN–TiC–TiN coated carbide inserts (ISO P45-M35 class) under dry machining conditions. Focus of their research was to determine the best set of processing parameters that yield the fastest convergence for the coefficients of the extended Taylor tool life equation using the minimum ratio between minimum and maximum singular values of the sensitivity matrix of tool life related to variation of parameters. It was pointed out in their study that the mean percentage error in tool life estimates for AISI 304 stainless steel was 46% compared to 10% for AISI 1045 steel under similar cutting conditions. Irregular flank wear patterns and variations in work-piece material composition in AISI 304 stainless steel caused higher variations in tool life estimates compared to AISI 1045 steel. Sharman et al. (2001) studied tool life for high-speed ball nose end-milling of Inconel 718 alloy with TiAlN and CrN coated carbide inserts under dry machining conditions. From their experiment where two levels (high and low) of work piece angle, cutting speed and coating material were tested, they established a relationship between maximum flank wear (0.3 mm) and processing parameters. The result from the experiment showed that tool coating was the main factor that affected tool life most significantly, followed by cutting speed, and work piece angle.

It can be seen from the above studies that tool wear in end-milling under dry and semi-dry machining conditions is mainly predicted using regression modeling technique. One of the major problems associated with tool wear modeling of end-milling under such machining conditions is the prevalence of non-uniform tool wear and notch wear (Alauddin and El Baradie, 1997; Alauddin et al., 1995; Dos Santos et al., 1999; Sharman et al., 2001). Under such conditions, tools interact with work piece material at high temperatures resulting in the development of non-uniform wear caused by adhesion, diffusion and chemical wear. Non-uniform wear causes work piece hardening and variation in composition at the surface. In addition, excessive tool deflection causes vibration and chattering that can promote notching. These sources of variation can lead to large error terms in ordinary regression models such as the ones which have been previously utilized for tool wear modeling. A common strategy to counteract this effect has been to repeat tool wear experiments anywhere from two to five times or more in order to obtain an average wear value (Alauddin and El Baradie, 1997; Alauddin et al., 1995; Sharman et al., 2001). However, as a result of this practice, the tool wear model may fail to detect significant effects because of decreased statistical power. Furthermore, the inference based on the averaged observations does not reflect the true variability inherent in the process and may lead to false conclusions. To overcome the limitation of ordinary regression approaches, this paper considers a different modeling technique for tool wear progression for end-milling under dry and semi-dry machining conditions, called the mixed effects model.

2. Mixed effects modeling technique and the experimental details

2.1. *Mixed effects modeling technique*

Since its first introduction by Laird and Ware (1982), mixed effect models have been used in reliability and survival analysis extensively. This modeling technique has also been endorsed in a reliability context since it has been recognized that measurements over time can provide more information compared to single life time measurements in circumstances where a reliable marker exists (Meeker and Escobar, 1998).

A two-stage approach is inherent to the mixed effects modeling technique. In the first stage, patterns in longitudinal measurements are captured using subject specific regression coefficients incorporating known factors or covariates. Note that linear or non-linear regression models may be used in this stage. In the second stage, subject specific parameters are related to the known covariates using multiple regression models (Onar et al., 2006). There are many studies utilizing mixed effects modeling in engineering, statistics and reliability in the literature (Onar et al., 2006; Carey and Koenig, 1991; Doksum and Holyland, 1992; Lawless et al., 1995; Kwam and Bae, 2004).

In the simplest case, the linear mixed effects model utilizes linear regression, $\mathbf{Y}_i = Z_i\boldsymbol{\theta}_i + \boldsymbol{\varepsilon}_i$, in the first stage to represent the specimen-specific longitudinal measurements; and relates the specimen-specific parameter vector, $\boldsymbol{\theta}_i$ to the known covariates via $\boldsymbol{\theta}_i = K_i\boldsymbol{\beta} + \mathbf{b}_i$ in the second stage. Combining these two stages together leads to

$$\mathbf{Y}_i = Z_i(K_i\boldsymbol{\beta} + \mathbf{b}_i) + \boldsymbol{\varepsilon}_i = (Z_iK_i)\boldsymbol{\beta} + Z_i\mathbf{b}_i + \boldsymbol{\varepsilon}_i = X_i\boldsymbol{\beta} + Z_i\mathbf{b}_i + \boldsymbol{\varepsilon}_i \quad (1)$$

where $\mathbf{b}_i \sim N(0, D)$, $\boldsymbol{\varepsilon}_i \sim N(0, \Sigma_i)$, $b_1, b_2, \ldots, b_n, \varepsilon_1, \varepsilon_2, \ldots, \varepsilon_N$ are independent of each other; and $X_i = Z_iK_i$; $\mathbf{Y}_i = n_i$ dimensional response vector of subject i, for $1 \le i \le N$; N: number of subjects; Z_i: $n_i \times q$ and K_i: $q \times p$ are matrices of known covariates; $\boldsymbol{\theta}_i$: specimen-specific parameter vector for subject i; $\boldsymbol{\beta}$: p dimen-

sional vector containing fixed effects; $\mathbf{b}_i$: q dimensional vector containing the random effects subject i; $\boldsymbol{\epsilon}_i$: n_i dimensional vector of residual components subject i; $D = [q \times q]$ covariance matrix; $\Sigma_i = [n_i \times n_i]$ covariance matrix which typically depends on subject i only through its dimension n_i, i.e. the set of unknown parameters in Σ_i will not depend on i. In some cases, this assumption is relaxed (Verbeke and Molenberghs, 1999).

This modeling technique is known for its versatility and can also be used in cases where measures are unequally spaced or when sample sizes across units are unequal. Mixed effects models are particularly useful when there are unobserved and/or uncontrolled subject specific variations which may affect the response of interest. In a metal cutting context, such variations include material composition, work piece hardness and other source of machining variations which may or may not be observable.

2.2. *Design of the experiment*

An experiment was designed using four independent variables; cutting speed (two levels), feed rate (three levels), depth of cut (two levels) and cutting condition (two levels). A full factorial design was selected to facilitate the estimation of all main and interaction effects. Twenty-four treatment combinations each with two replications were run in a random order. The selection of test blocks for the experimental runs was also randomized. Levels for the independent variables were selected to cover the cutting range of the insert as recommended by the manufacturer (Kennametal). Two levels of cutting speed were selected in the upper speed range (183 m/min and 229 m/min) in order to ensure that the insert reached its flank wear criterion within the confines of the test block used for the experiment. Also, a higher cutting speed yields higher rate of material removal. Similarly three levels were selected for feed rate (0.10 mm/rev, 0.15 mm/rev, and 0.20 mm/rev) to cover the manufacturer recommended feed range for the insert. Two levels were selected for depth of cut (DOC) (2.54 mm and 3.81 mm): the lower level was selected to ensure that the end-milling insert reached its wear criterion within the confines of the test block; whereas the higher level was chosen at a depth of cut less than half of the insert cutting edge length to prevent accidental breakage of the insert during end-milling. Semi-dry and dry were selected as the two cutting conditions. Each experimental combination was repeated twice to capture experimental error for the mixed effects modeling of tool wear progression. The variables that were kept constant throughout the experiment were work piece material (composition and size), tool geometry (rake angle, hone, T land, and finish), machine and operator. Note that even though in a typical case a factorial design implies one observation per cutting condition, we obtained serial measurements throughout the life time of the insert in an effort to capture the tool wear patterns under our experimental conditions. After the initial reading taken following the 2nd cut, flank wear readings were generally recorded every four cuts till the block reached its wear criterion.

2.3. *Details of the experiment*

An Okuma vertical machining center (VMC Model ES-V3016) was used for the experiment. This machining center has a nominal spindle power rating of 7.4 HP (5.5 KW) and is fit-

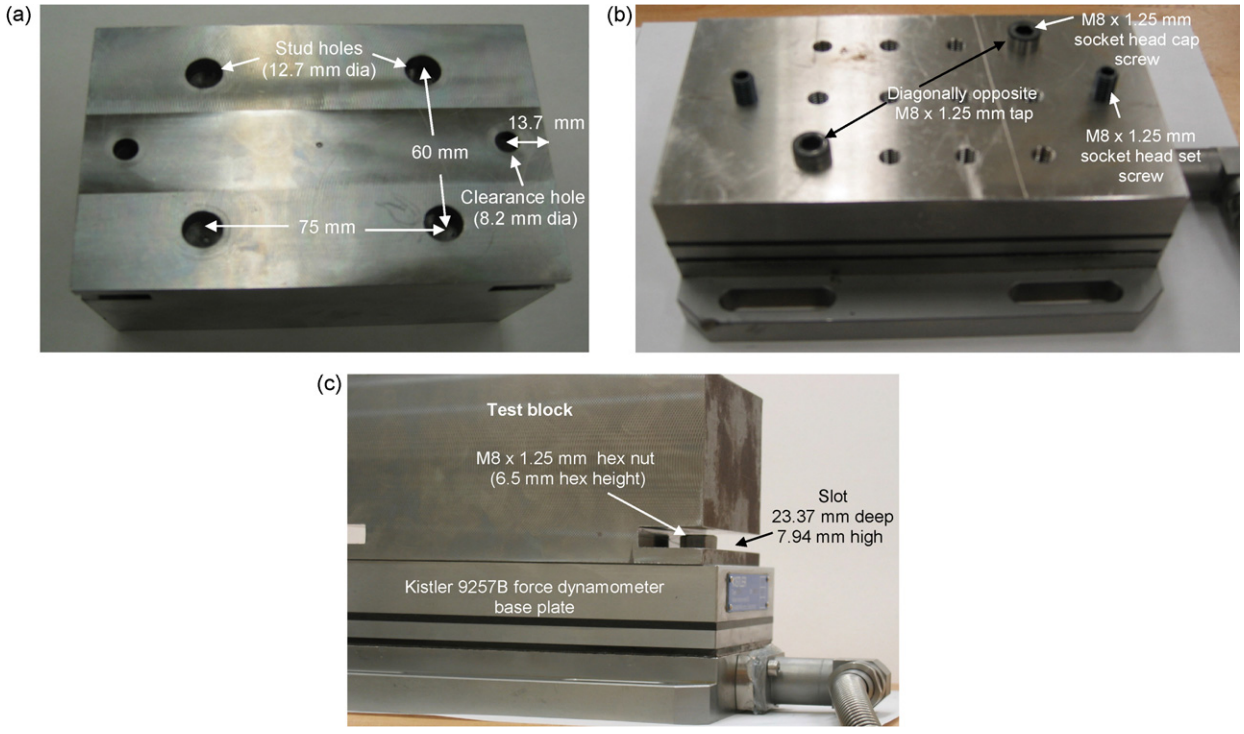

Fig. 1 – (a) Location of stud and clearance holes on bottom of test block, (b) location of socket head cap screw and socket head set screw on Kistler force dynamometer (Type- 9257B) base plate, and (c) assembly of test block on Kistler dynamometer base plate.

ted with a CAT 40 V flange tapered shank. Physical vapor deposited (PVD) multi-layer TiAlN–TiN coated Kennametal KC725M grade carbide 10 mm IC end-milling inserts were selected for the study (ISO designation of SPET10T3PPERGB). The insert thickness is 3.96 mm with an overall coating thickness in the range of 3–5 μm. The substrate material consists of tungsten carbide with an 11.5% cobalt binder. The tough PVD coating material and the thermal shock resistance of the substrate makes this insert suitable for both semi-dry and dry machining applications. The square insert has a rake and end relief angle of 5°, a clearance angle of 11°, a medium honed cutting edge (length 10 mm) and an edge radius of 0.79 mm. A Kennametal single insert tool holder (KISR-KSSM 10 mm IC) with a CV40 shank and an effective cutting diameter of 19 mm was used to hold the insert during machining.

Normalized and tempered AISI 4340 medium carbon low alloy steel blocks with an average hardness of 26 HRc was used for the experiment. This alloy steel is widely used in the fabrication of machine tool structural parts, power transmission gears and shafts in the automotive industry, and aircraft landing gears parts. Each test block was 152.4 mm long, 101.6 mm wide, and 76.2 mm high. Four stud holes (12.7 mm diameter) were drilled and reamed to a depth of 7.62 mm at the bottom of each test block in a rectangular pattern as shown in Fig. 1(a). A 7.94 mm high, 23.37 mm slot was machined at a height of 6.35 mm from the bottom of the test block on either side. Two clearance holes of diameter 8.2 mm were also drilled through the middle of the slotted section of the block. The bottom of the blocks were deburred and lapped to obtain a tight fit with the base plate of a Kistler make three-component dynamometer (Type 9257B). It is to be noted that force readings obtained from the dynamometer were not used in this study. The dynamometer was used to hold the test block for machining. Two M8 × 1.25 mm socket head cap

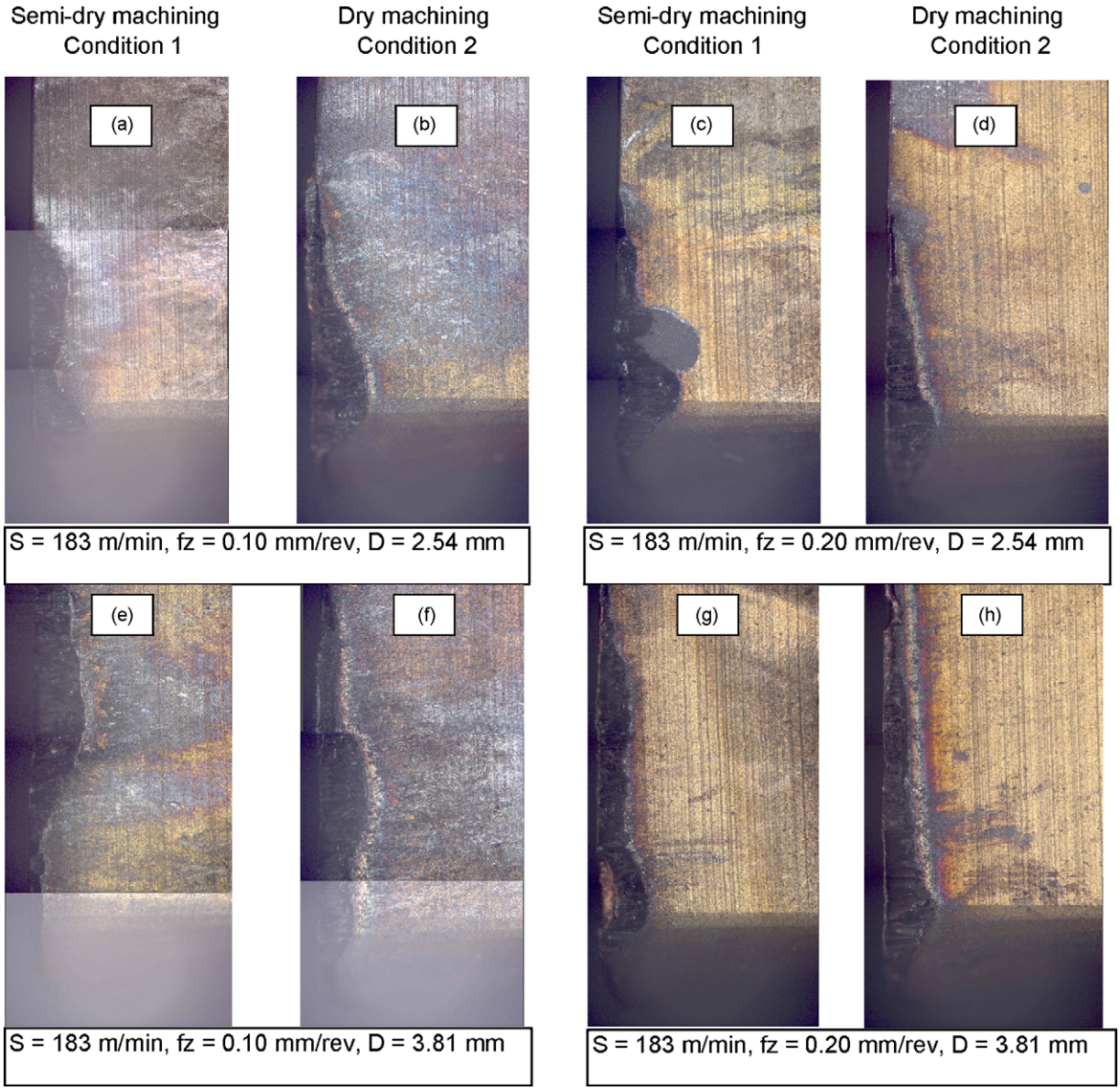

Fig. 2 – Worn out flank face of PVD TiAlN–TiN multi-layer coated carbide tools after the insert reached its flank wear criterion of 0.40 mm (400 μm).

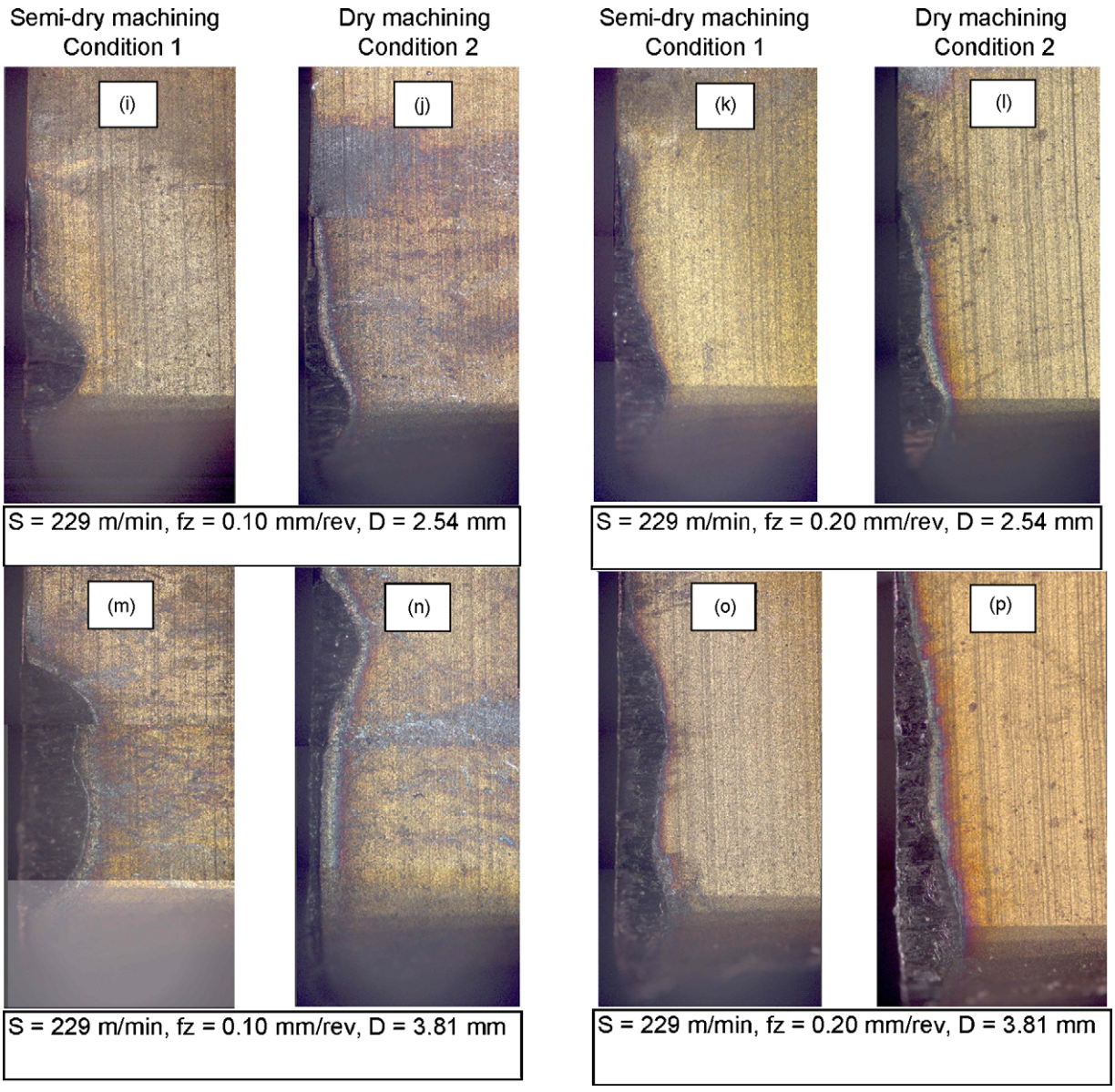

Fig. 2 – *Continued*.

screws (material: alloy steel—grade 8) were machined to fit into two diagonal M8 × 1.25 mm blind tap holes (10 mm deep) located on the dynamometer base plate as shown in Fig. 1(b). The diameter of the socket head was machined on a lathe to 12.7 mm for it to make a tight fit with the corresponding stud holes located at the bottom of the test block. The blocks were anchored down to the dynamometer base plate using M8 × 1.25 mm socket head set screws (20 mm in length, material: alloy steel—grade 8) and M8 × 1.25 mm hex nuts (material: stainless steel—A4) having 6.5 mm hex height as shown in Fig. 1(c). This ensured a tight and secure grip of the test block to the dynamometer. The dynamometer with the test block attached to it was then clamped on a Kurt make precision part clamping vise (AngLock® D-Series, Model - D675) that was bolted to the table of the Okuma machining center. This setup kept machining vibrations at a minimum level. Vibration is one source of variation in the machining process that can introduce errors in the tool wear progression model.

An optical microscope (Carl Zeiss make) was used to measure flank wear. Wear readings were generally taken every four subsequent cuts till the insert reached its flank wear criterion (400 μm) for each treatment combination. A misting device was used to dispense 757 ml/h of water soluble coolant at a pressure of 0.65 MPa for semi-dry machining conditions. A 100% water-soluble synthetic and bio-degradable mist coolant (Kool MIST™ Formula #78) was used. The mix ratio used was 113 g of coolant concentrate in 3.8 l of water. Hardness of test pieces before and after machining was measured using a Wilson make bench hardness tester. Hardness of each machined layer was recorded using a portable hardness tester (Mitutoyo Hardmatic HH-401).

The length of each cut was equal to the length of the test block (i.e. 152.4 mm). A cutter immersion ratio of 2/3 was used for the experiment. Prior to initiating the full experiment, a pilot study was conducted to confirm that the combinations of the lowest levels of all cutting parameters selected caused the insert to reach its flank wear criterion within the confines of the test block. It was observed that non-uniform flank wear prevailed on the flank face of the insert (Fig. 2). Maximum flank wear was thus selected as the preferred mode of failure of the insert. ISO 8688-2: 1989 (E) specifies a recommended uniform wear criterion of 0.3 mm or a maximum wear criterion of 0.5 mm when machining steel during end-milling applications (Tool Life Testing in Milling—Part 2: End-milling, International Standard, 1989). A maximum flank wear criterion of 0.5 mm can cause catastrophic failure of the insert and damage the tool holder and was thus not selected as the wear criterion in this study. Instead the tool life criterion was set at a safe level of 0.4 mm (or 400 μm) based on recommendations from the insert manufacturer.

3. Results and discussion

3.1. *Model fitting*

As a first step of the modeling process, data plots were obtained for progression of flank wear for individual blocks. Fig. 3 shows the non-linear relationship between flank wear (Wear in micrometer) and cut number (Cut no). In the absence

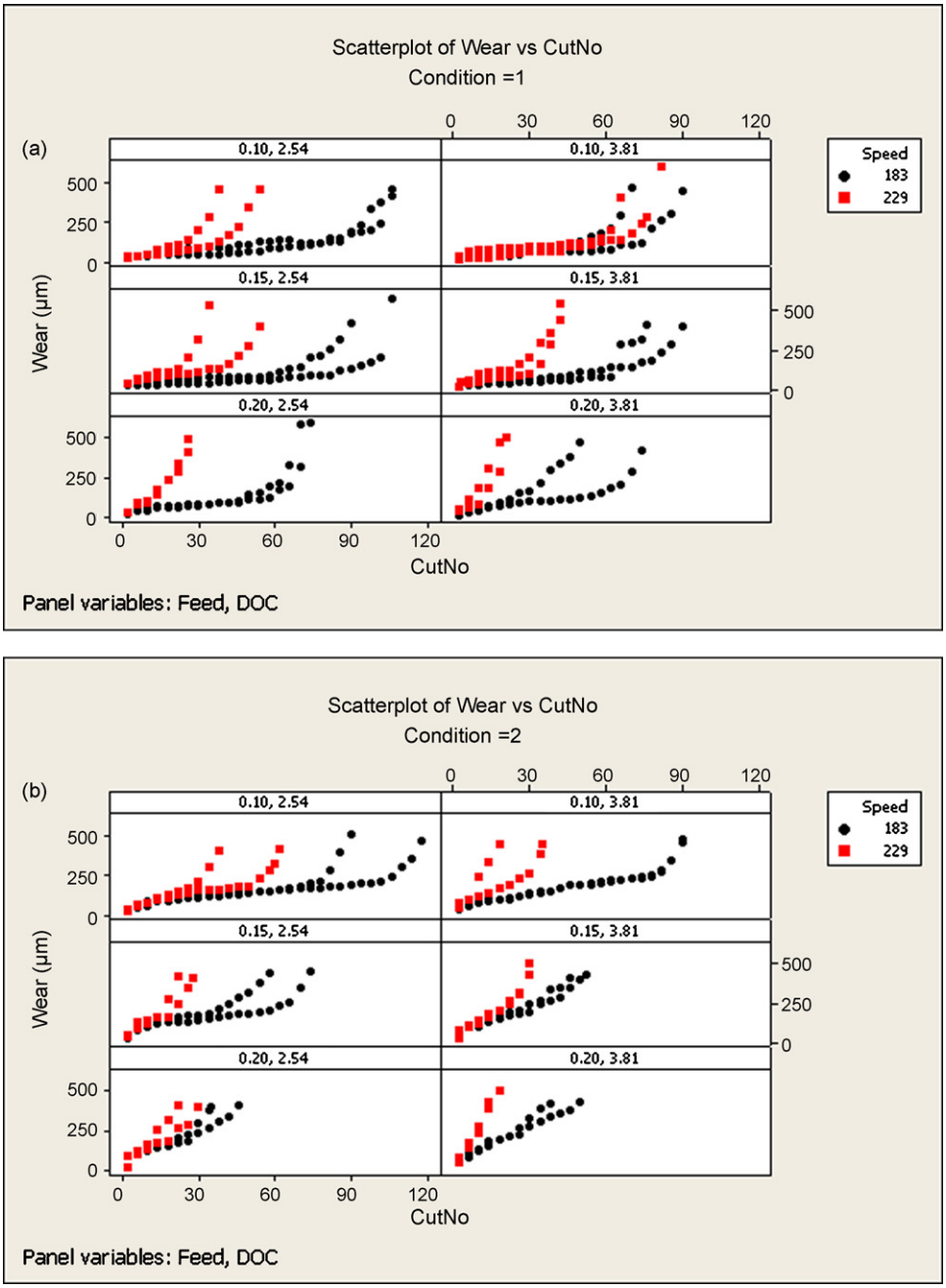

Fig. 3 – Scatter plot of flank wear in micrometer versus cut number (Cut no.) under (a) semi-dry (Condition 1), (b) dry machining conditions (Condition 2).

of a mechanistic argument, it is not advisable to fit a non-linear model purely based on empirical data (Onar et al., 2006). In order to reduce the non-linearity in the profiles as well as normalize the residuals, a Box–Cox transformation (Box and Cox, 1964) as implemented in Minitab Release 14 was utilized, which suggested natural log as the most suitable transformation. Fig. 4 shows the scatter plots of natural log of wear versus number of cuts. It can be noted from the plots that the transformation is not adequate to achieve the desired linearity and thus a polynomial of the third degree was employed to capture the relationship between ln Wear and Cut no.

S-Plus 2000 statistical software package was used to fit the best yet the simplest cubic model to the transformed data of the individual wear progression profiles. During the model fitting process, various residual plots were monitored to check for departures from model assumptions such as non-constant variance, non-linearity in the residuals, non-normality or substantial auto-correlations associated with consecutive observations.

Akaike information criterion (AIC) and Bayesian (Schwarz) information criterion (BIC) goodness-of-fit statistics as generated by S-Plus were used to compare different models during the model fitting process. These criteria penalize for the number of terms in the model as per the parsimony principle, i.e. keep least number of entities (in a similar way that the R^2 adjusted works in a multiple regression setting) (Onar et al., 2006). Smaller values of AIC and BIC criterion indicate a better model fit. However, these values have to be considered in

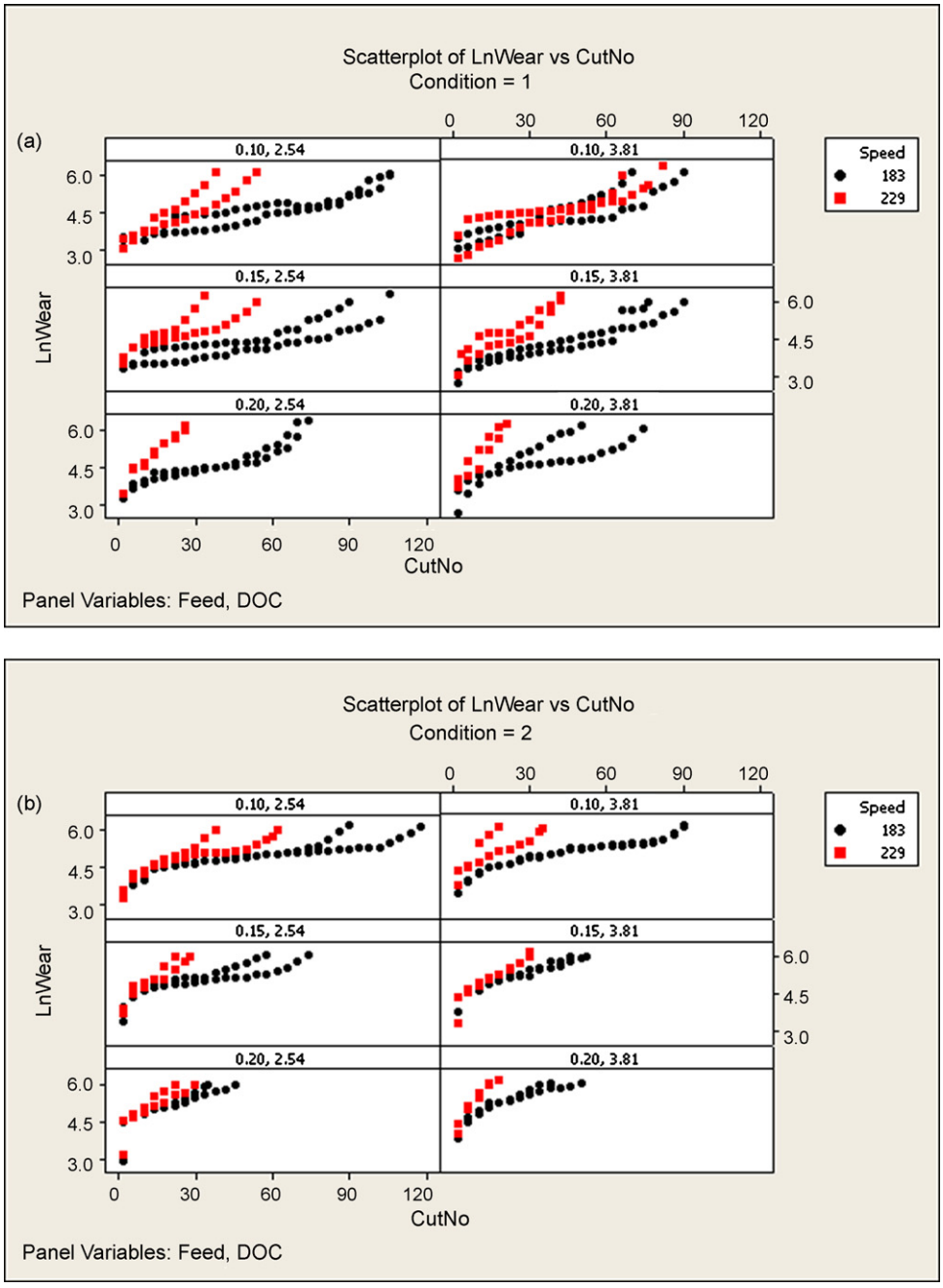

Fig. 4 – Scatter plot of ln Wear versus Cut no. under (a) semi-dry (Condition 1), (b) dry machining conditions (Condition 2).

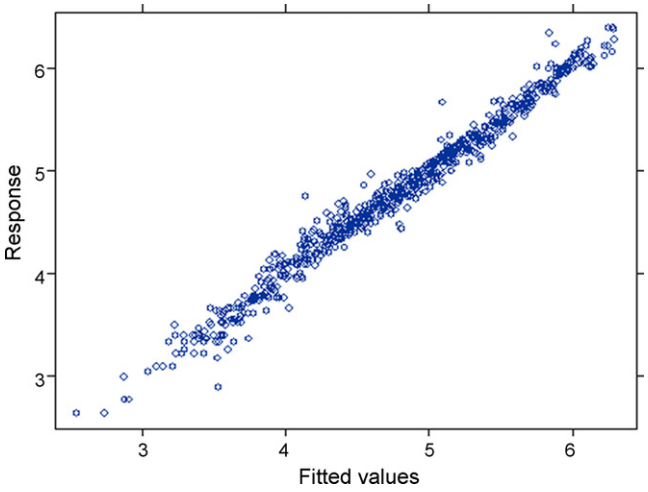

Fig. 5 – Response versus fitted value plot of the model.

conjunction with various residual plots mentioned earlier to determine the best model fit. It should be noted however that these values cannot be used if one is interested in comparing models based on dependent variables measured on different scales.

Starting with the full cubic model (including all 2, 3, and 4-way interactions of the experimental variables) and using a backward elimination approach aided by residual plots as well as the above mentioned goodness-of-fit criteria, the following mixed effects model was selected for flank wear progression:

$$\begin{aligned}\ln \text{Wear} = {} & 2.709441 + 0.045327\text{Speed}_I + 0.313842\text{Feed}_{0.15} \\ & + 0.678739\text{Condition}_I + 0.595547\text{Feed}_{0.2} \\ & + 0.092218\text{Cut no.} - 0.002151\text{Cut no.}^2 \\ & + 0.000021\text{Cut no.}^3 + 0.069427\text{Speed}_I\text{Cut no.} \\ & - 0.002645\text{Speed}_I\text{Cut no.}^2 + 0.000048\text{Speed}_I\text{Cut no.}^3 \end{aligned} \quad (2)$$

Indicator variables were chosen for speed, feed, depth of cut, and cutting condition as the wear progression curves obtained are specific to these levels selected. Treating speed and feed as continuous data was deemed inappropriate since such an approach would require extrapolation in regions where no data was collected. The indicator variables for speed, depth of cut, and cutting condition were coded as Speed_I, DOC_I, and Condition_I respectively. For the two levels, the smaller value was coded as 0 and the larger value coded as 1. The coefficients for these terms represent the change that can be expected when one moves from level 0 to level 1, i.e. from the lower level to the higher level. Feed had three levels that were modeled by using two indicator variables, namely $\text{Feed}_{0.15}$ and $\text{Feed}_{0.2}$. In each case, the coefficients for these variables were compared to their baseline value, i.e. the $\text{Feed}_{0.1}$ level. The response versus fitted value plot is shown in Fig. 5 which indicates a very good model fit to the wear progression data. It was observed that the curvature, as captured by the cubic model of ln Wear versus Cut no. graph (Fig. 4) is mainly affected by speed and thus the interaction of speed with linear, quadratic, and cubic terms of Cut no. have been included in the model. As can be seen from Eq. (2), the model incorporates the effect of cutting speed, feed, cutting condition and cut number on flank wear. Depth of cut did not have a significant effect on flank wear progression in this study. The lack-of-notable effect of DOC can also be observed graphically by comparing the left column with the right column in Fig. 4(a) and (b). There is no indication in these plots that a significant change in slope of the ln Wear versus Cut no. curve occurs when DOC is changed from 2.54 mm to 3.81 mm across the cutting combinations selected. In contrast, a notable change in the shape of the curves is observed when cutting speed and feed levels are changed. It is to be noted that the mixed effects model shown in Eq. (2) does not include any speed and feed interaction term as they were not statistically significant in this case. Figs. 3 and 4 clearly display that these interactions are not all that influential as the only clear separation observed from these plots is due to speed. The simpler model is being proposed as it is much easier to interpret, yet retains all statistically significant variables.

3.2. *Hardness variation in workpiece*

As mentioned earlier, one of the sources of between and within block variations is test block hardness. The surface hardness of the work piece initially increased due to work hardening of the machined surface during both semi-dry and dry machining operation and subsequently decreased as successive cuts exposed inner layers of the blocks that were comparatively softer. Fig. 6 shows the variation of the surface hardness of a typical AISI 4340 alloy steel work piece (block # 21) from initial un-machined surface (surface # 1) to the final surface (surface # 7) before the flank wear criterion was reached. It is noted here that tool wear models developed in the majority of metal cutting literature assume that work pieces have homogeneous chemical composition and hardness. As seen from hardness measurements done during the experiment in this study, this assumption may not always be true. Hardness measurements obtained before and after end-milling indicated variation across test blocks (Table 1).

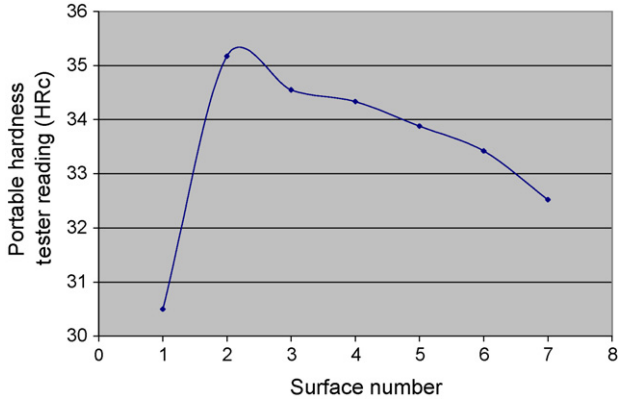

Fig. 6 – Variation in surface hardness of block 21 used for machining under a cutting speed of 183 m/min, feed rate of 0.15 mm/rev, a depth of cut of 3.81 mm under dry machining condition.

Table 1 – Summary of hardness measurement of initial and final layer for the forty eight AISI 4340 alloy steel blocks used for the experiment

Test block number	Hardness measurement (Rockwell—HRc)			
	First layer (un-machined surface)		Last layer (machined surface)	
	Bench top tester	Portable tester	Bench top tester	Portable tester
Mean	26.2	25.6	34.3	33.4
Min	21.3	20.8	32.6	30.1
Max	31.3	30.5	36.7	35.8
S.D.	2.48	2.47	1.08	1.40

Table 2 – Parameter estimates for the mixed effects model with associated *p* values*

Terms	Value	S.E.	Degree of freedom (d.f.)	*t*-Value	*p*-Value
Intercept	**2.709441**	**0.109888**	**634**	**24.65638**	**<0.0001**
$Speed_I$	0.045327	0.1235976	43	0.36673	0.7156
$Feed_{0.15}$	**0.313842**	**0.0950245**	**43**	**3.30275**	**0.0019**
$Condition_I$	**0.678739**	**0.0778535**	**43**	**8.71816**	**<0.0001**
$Feed_{0.2}$	**0.595547**	**0.0955489**	**43**	**6.2329**	**<0.0001**
Cut no.	**0.092218**	**0.0113641**	**634**	**8.11486**	**<0.0001**
I(Cut no.^{2})	**−0.002151**	**0.000359**	**634**	**−5.98998**	**<0.0001**
I(Cut no.^{3})	**0.000021**	**0.0000048**	**634**	**4.42299**	**<0.0001**
$Speed_I$:Cut no.	**0.069427**	**0.0166875**	**634**	**4.16041**	**<0.0001**
$Speed_I$:I(Cut no.^{2})	**−0.002645**	**0.0005721**	**634**	**−4.62236**	**<0.0001**
$Speed_I$:I(Cut no.^{3})	**0.000048**	**0.0000082**	**634**	**5.77437**	**<0.0001**

* Significant terms at 95% confidence level have been shown in bold.

Although a request was made to the AISI 4340 steel block supplier to ensure uniform hardness, variations in hardness measurements before and after machining was still observed. The mixed effects modeling technique incorporates a set of subject-specific random effects that take into account unobserved heterogeneity, part of which is caused by material hardness variation.

3.3. *Interpretation of model coefficients*

The 2nd column labeled "Value" in Table 2 shows the parameter estimates of the model. The last column in the table shows the associated *p*-values. It can be seen that indicator variables speed, feed, and condition were retained in the final mixed effects model. Following the parsimony principle, depth of cut was not included in the model as it did not improve the model fit. Among the main effects, the coefficient for $Condition_I$ was positive and highly significant (*p*-value <0.0001). This means that average initial wear values obtained under dry cutting conditions are expected to be higher than the average initial wear values under semi-dry cutting conditions, keeping all other variables the same. Similarly the coefficients of $Feed_{0.2}$ and $Feed_{0.15}$ terms were both positive and highly significant (*p*-values <0.0001 and 0.0019, respectively). The implication here is that keeping all else the same, changing feed levels from 0.10 mm/rev to 0.15 mm/rev or from 0.10 mm/rev to 0.20 mm/rev, the average initial wear values are expected to increase. It is to be noted that the effect of term $Speed_I$ (i.e. higher level of cutting speed) on initial wear value is not significant at 5% significance level; however $Speed_I$ is involved in interactions with Cut no. and was thus retained in the model.

3.4. *Effect of cutting speed on wear progression*

With respect to the rate of flank wear progression, it can be seen from Fig. 7 that a significantly higher rate of flank wear progression evidenced by a steeper wear progression curve is obtained with the higher cutting speed level (229 m/min). All three Cut no.–$Speed_I$ interaction parameters in Table 2 are highly significant (all *p*-values <0.0001) indicating that moving from lower to higher speed changes the overall shape of the wear progression curve. It would however not be appropriate to look at the magnitude of these interaction parameters and compare them to each other or to the main effects to infer their relative importance. This is because they are being multiplied by different orders of Cut no. and thus the scale associated

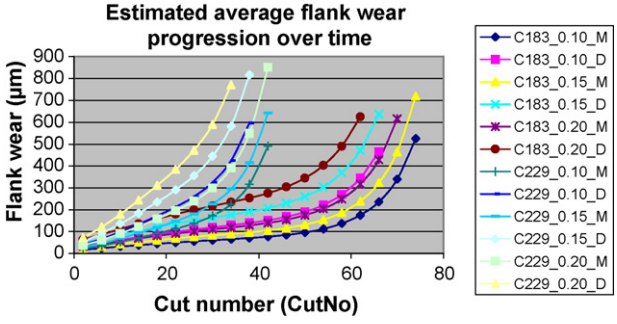

Fig. 7 – Plot of average estimated flank wear progression with number of cuts for mixed effects model (Notations: C183_.10_M; speed—183 m/min, feed—0.10 mm/rev, M—mist cutting condition.; D—dry cutting condition).

with each of them is different. It is observed however that at a higher cutting speed level of 229 m/min, the coefficients of the linear and cubic Cut no. terms combine together to form larger positive coefficients thus increasing the slope of the wear versus Cut no. progression curve. Therfore, at a higher speed level, the wear progression curves are much steeper compared to a lower cutting speed level of 183 m/min as seen in Fig. 7.

3.5. *Interpretation of standard deviation of random effects*

The standard deviations for the random effect terms are shown in Table 3. Though the interpretations are not as straight forward due to the presence of high correlations among the random effect terms, it can be seen that the standard deviation of the intercept random effect term, which represent the variability in block-specific adjustments from the overall intercept, is substantially higher (approximately 3.5 times) than the standard deviation of the error residual term. This indicates that the variation between blocks under similar cutting conditions is much larger compared to the within block variation as captured by the standard deviation of the residual error. Failing to capture the inter-block variation in this way would result in a substantially inflated residual error variance which in turn would have hindered the model's ability to detect significant effects. Table 3 also shows that there is a high correlation (−0.975) between linear and quadratic effects, and quadratic and cubic effects of Cut no. (−0.920). A correlation coefficient of 0.841 was observed between linear and cubic effects of Cut no. Also, moderately high correlation coefficient values were observed between intercept and linear, quadratic, and cubic terms of Cut no. The model allows the random effects to be correlated using the most general form of a disperion matrix, i.e. general positive definite matrix.

3.6. *Microscopic image of flank wear surface*

Images of worn out flank surface of the inserts were taken using a Zeiss "Axioskop 2 Mat" optical microscope. Fig. 2 shows the worn out flank surface of the insert after the tool reached its flank wear criterion of 0.40 mm or 400 μm. In all cases, non-uniform flank wear was observed. In general, no chipping of inserts was observed in this study under semi-dry or dry cutting conditions. The only exception occurred at a cutting speed of 183 m/min, feed rate of 0.20 mm/rev and depth of cut of 2.54 mm under semi-dry cutting conditions as seen in Fig. 2(c). The chipping may be attributed to higher feed rate and insert coating imperfections. Also, the maximum flank wear apparently looks higher for the semi-dry cutting condition in Fig. 2(m) compared to dry condition in Fig. 2(n) after the insert reached its wear criterion under a cutting speed of 229 m/min, feed rate of 0.10 mm/rev and depth of cut of 3.81 mm. This is because the image of the flank face of the insert was taken for cut # 82 when the flank wear reached 600 μm. The previously measured flank wear was 275 μm obtained at cut # 76. An attempt was made to stop machining once the flank wear criterion of 400 μm was reached. However, it was not always possible to stop the end-milling process at exactly 400 μm wear. This however did not pose a problem for modeling purposes as the mixed effects models can take into account unequally spaced readings or unequal sample sizes.

Table 3 – Estimates of the variance components of the random effect terms

Random effect	Standard deviation	Correlation matrix		
(Intercept)	0.40772743632	(Intercept)	Cut no	I(Cut no.^{2})
Cut no.	0.05388482331	−0.757		
I(Cut no.^{2})	0.00167926364	0.733	−0.975	
I(Cut no.^{3})	0.00002238862	−0.581	0.841	−0.920
Residual S.D.	**0.12484468916**			

3.7. *EDX analysis of crater surface of insert*

Electron dispersive X-ray (EDX) analysis of the crater surface of the insert was conducted to determine the nature of wear. The spectral information obtained from this analysis coupled with the knowledge of chemistry can be used to explain the type of wear that occurs at the crater face of the insert. Fig. 8(a) shows the EDX spectrum for a new insert. Titanium (Ti), aluminum (Al) and nitrogen (N) peaks can be prominently seen in the spectrum shown in the figure. These elements are the constituents of the TiAlN–TiN coating of the carbide insert used for the study. Fig. 8(b) and (c) show the EDX spectra of the crater surface of the worn out insert subjected to semi-dry and dry machining conditions respectively at a cutting speed of 229 m/min, feed rate of 0.20 mm/rev, and depth of cut of 3.81 mm. A comparison of the two spectra shows a higher iron (Fe) K_α peak obtained during dry machining conditions. This is an indication of an iron built up edge that occurs during dry machining. Other elemental peaks that show up in the spectra of the worn out inserts are oxygen (O), carbon (C), silicon (Si), tungsten (W) L_α and M_α peaks, titanium (Ti) K_α and K_β peaks, chromium (Cr), manganese (Mn) and nickel (Ni). The elements mentioned above are alloying elements in AISI 4340 steel used for the experiment. Diffusion wear at the tool-chip interface cause the material transfer from the work piece to the insert crater surface. This type of wear occurs at the tool-work piece interface at temperatures in the range of 700 °C to 900 °C. During the diffusion process, metal and carbon particles migrate into the stream of work piece material flowing past the insert crater surface in the form of chips generated during the machining process. At the same time, atoms of alloying elements present in the work piece material diffuse onto the insert crater surface or react with the insert coating to degrade it further (Trent, 1991).

A higher level of oxygen was also detected on the crater surface of the insert used in dry machining indicating the presence of oxide layers on the surface. Oxidation during dry machining is also aided by the fact that titanium carbide (TiC) and tungsten carbide (WC) have a higher tendency to oxidize. It is to be noted that oxide layers form on carbide tools at a temperature range of 900 °C (Rahman et al., 2002). It can thus be inferred that the tool crater surface is subjected to high temperatures in this range during dry machining conditions. Oxide layers are also formed during semi-dry machining as shown in Fig. 8 (b) but to a lesser extent. The coolant mist

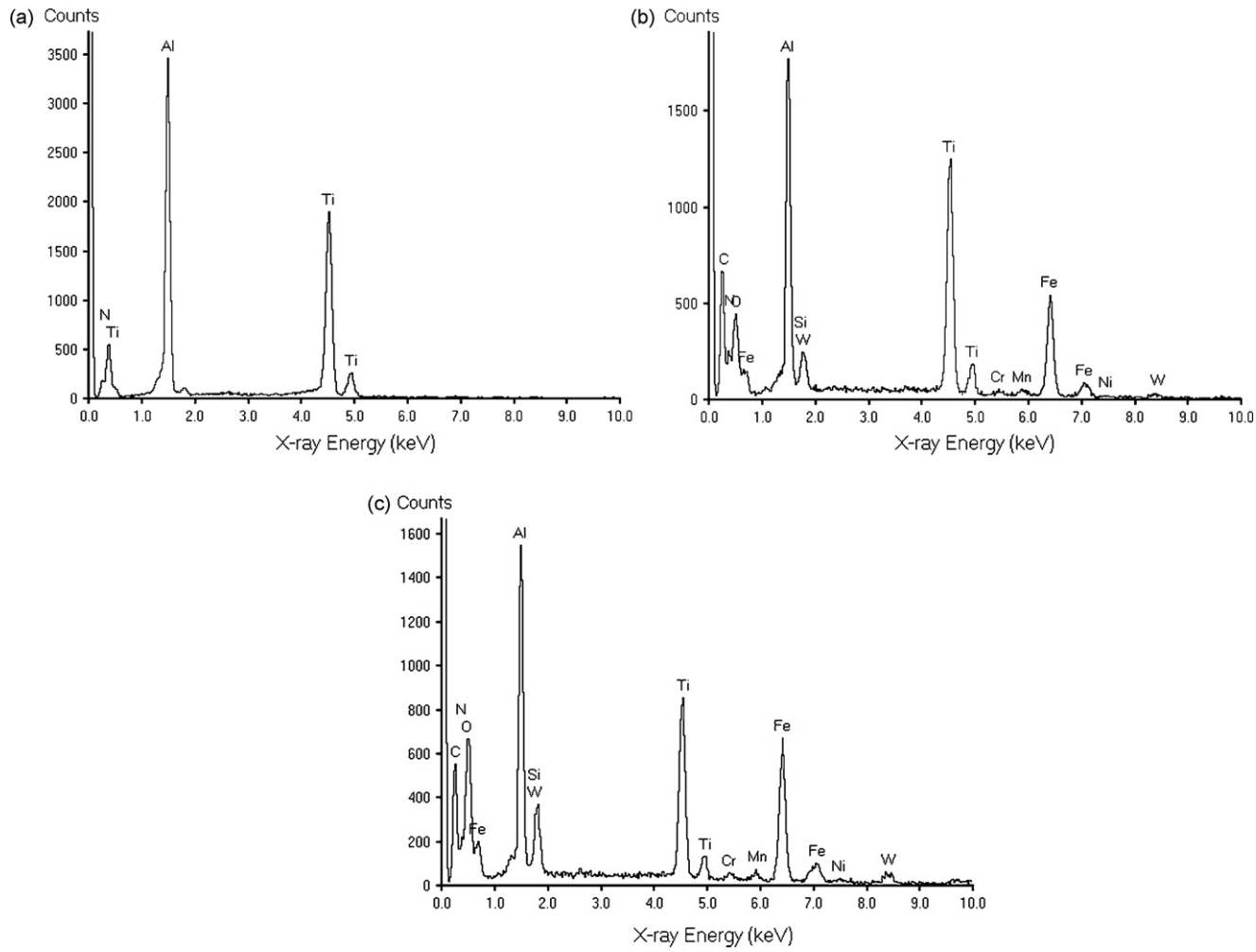

Fig. 8 – Energy dispersive X-ray (EDX) spectra obtained for the rake face of the coated carbide insert (a) brand new, (b) after the insert reached the wear criterion under semi-dry machining conditions, and (c) after the insert reached the wear criterion under dry machining conditions (cutting speed—229 m/min, feed rate—0.20 mm/rev, DOC—3.81 mm).

used in semi-dry machining shields the tool/work piece interface from direct exposure to oxygen in air, thus lowering the tendency of TiC and WC to oxidize.

3.8. *Backscatter image analysis*

Primary and secondary backscatter images of the crater surface of worn out inserts were obtained using environmental scanning electron microscopy (ESEM) after they reached their wear criterion. Fig. 9(a) and (b) show backscatter electron images of the crater surface of the insert subjected to a cutting speed of 229 m/min, feed rate of 0.20 mm/rev and depth of cut of 3.81 mm under semi-dry and dry cutting conditions. The backscatter image provides valuable information about the elemental composition of the crater surface as it is atomic number dependant. Elements with higher atomic numbers appear brighter in the backscatter image. As it can be seen in Fig. 9(a), the dark patch on the crater surface is the actual TiAlN–TiN coating material. The bright spot on the backscatter image corresponds to tungsten carbide (WC) substrate material exposed. The gray patch towards the top edge of the insert is built up edge material primary composed of iron oxide (Fe_3O_4). Under dry machining conditions, the TiAlN–TiN coating layer gets eroded due to diffusion wear that takes places on the crater face of the coated carbide insert at high cutting temperatures. This exposes the tungsten carbide (WC) substrate layer underneath over time. The higher level of diffusion wear in dry machining exposes more substrate tungsten carbide material, as shown by the bright spots in the backscatter image of the insert as seen in Fig. 9(b). This can also be verified from the higher elemental tungsten M_α peak obtained during dry machining as seen in Fig. 8(c). In addition, a higher level of iron oxide compound was detected on the crater face of the insert during dry machining. This is indicated by the higher presence of gray patches (Fe_3O_4 built up layer) and fewer dark patches (TiAlN–TiN coating material) on the crater surface during dry machining conditions as seen in Fig. 9(b). The same inference can be drawn from the EDX spectral images shown in Fig. 8(c). Higher (Ti) and (Al) K_α peaks are observed during semi-dry machining compared to dry machining conditions which can be attributed to a lesser degree of TiAlN–TiN coating wear (Chakraborty, 2007).

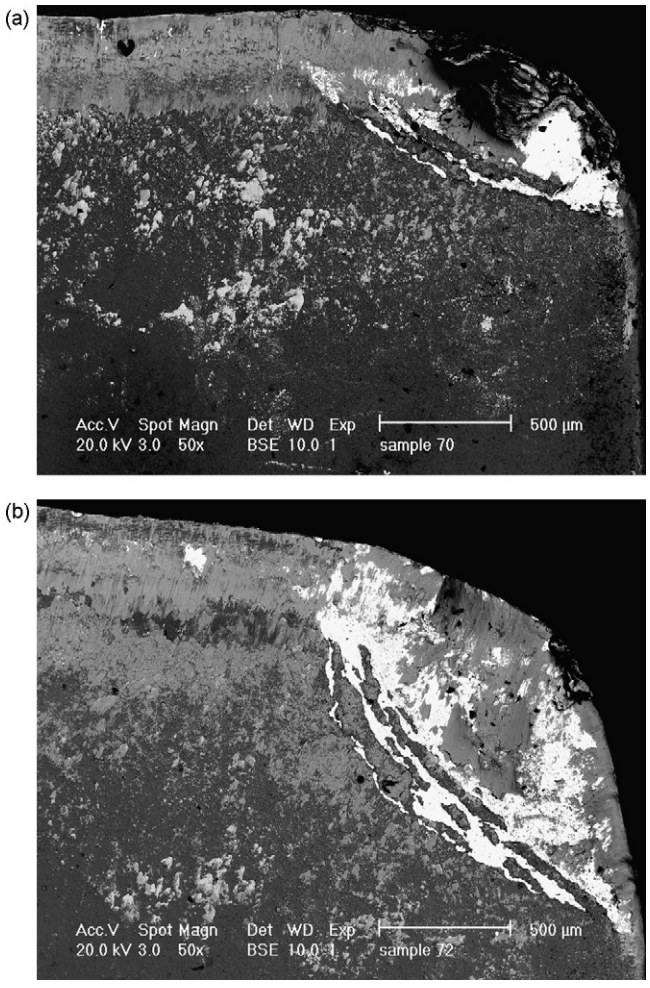

Fig. 9 – Backscattered electron image of the worn out crater face of coated carbide insert under (a) semi-dry, and (b) dry machining conditions (cutting speed—229 m/min, feed rate—0.20 mm/rev, DOC—3.81 mm).

4. Conclusion

A full factorial experiment was conducted with two replications for each treatment combination where longitudinal tool wear measurements were obtained. The resulting data was analyzed via a mixed effects technique which led to the development of a model describing tool wear progression during end-milling of AISI 4340 steel with PVD TiAlN–TiN coated inserts under dry and semi-dry machining conditions. To the best of our knowledge, this is the first application of the mixed effects modeling technique in metal cutting literature. This technique is suited for tool wear modeling in end-milling, especially under semi-dry and dry cutting conditions that involve variation in surface hardness and other sources of machining variations that can affect model accuracy. As stated before, mixed effects modeling technique takes into account variations between blocks as well as within blocks.

From the experiment, it is observed that the lowest initial wear value is obtained when using a cutting speed of 183 m/min, a feed rate of 0.10 mm/rev under semi-dry cutting conditions. From the model developed, it is also observed that cutting speed has the most comprehensive effect on tool wear progression in this study. A steeper slope of wear progression and a lower tool life is obtained at the higher cutting speed of 229 m/min compared to the lower cutting speed of 183 m/min. Though depth of cut was considered as a potential factor, the data collected did not provide adequate evidence corroborating this variable's effect on wear progression when it was studied in conjunction with other factors. The major advantage of the mixed effects approach to tool manufacturers will be reduction in the number of repetitions (usually 2–5 or more) in tool wear modeling experiments. Since the model takes into account both inter- and intra-block variability due to unobserved or uncontrolled variables such as hardness variation in work pieces, the data can be used more efficiently which typically would lead to a more accurate model of wear progression with fewer replications of each treatment combination compared to studies where conventional regression approaches are used. This can lead to substantial cost savings in procurement of test blocks that are used for similar wear experiments. Observing inter-block variability in the wear progression curves even for blocks which are studied under identical conditions can be very informative in determining how much inherent variability is present in the process.

EDX and backscattered electron images of the worn out coated carbide insert showed that diffusion wear prevails during end-milling of AISI 4340 steel under dry and semi-dry cutting conditions. A higher level of this type of wear occurs during dry machining.

Future research can focus on applying the mixed effects modeling technique to orthogonal machining as well in order to obtain accurate tool wear models at a reduced cost of running experiments. Tool wear models for end-milling using other material work piece-combinations using alternative cooling techniques like compressed chilly air or oil mist can also be developed.

Acknowledgement

The authors would like to thank Kennametal USA for supplying the PVD multi-layer coated carbide inserts used for this study.

REFERENCES

Alauddin, M., El Baradie, M.A., 1997. Tool life model for end-milling steel (190 BHN). J. Mater. Process. Technol. 68, 50–59.

Alauddin, M., El Baradie, M.A., Hashmi, M.S.J., 1995. Tool life testing in the end-milling of Inconel 718. J. Mater. Process. Technol. 55, 321–330.

Autret, R., Liang, S.Y., 2003. Minimum quantity lubrication in finish hard turning. In: Proceedings of International Conference on Humanoid, Nano Technology, Information Technology, Communication and Control, Environment, and Management (HNICEM), 2003, pp. 1–9.

Box, G.E.P., Cox, D.R., 1964. An analysis of transformations (with discussion). J. R. Stat. Soc. Ser. B (Methodol.) 26 (2), 211–252.

Carey, M.B., Koenig, R.H., 1991. Reliability assessment based on accelerated degradation: a case study. IEEE Trans. Reliab. 40, 499–506.

Chakraborty, P., 2007. Tool life and flank wear modeling of physical vapor deposited titanium aluminum/titanium nitride multilayer coated carbide inserts when end-milling 4340 steel under dry and semi-dry cutting conditions, Dissertation, University of Miami.

What you need to know about occupational exposure to metal working fluids, 1998. DHHS (NIOSH) Pub. No. 98–116.

Doksum, K.A., Holyland, A., 1992. Models for variable-stress accelerated life testing experiment based on Weiner processes and the inverse Gaussian distribution. Technometrics 34, 74–82.

Dos Santos, A.L.B., Duarte, M.A.V., Abrao, A.M., Machado, A.R., 1999. An optimization procedure to determine the coefficients of the extended Taylor's equation in machining. Int. J. Mach. Tools Manuf. 39, 17–31.

Tool Life Testing in Milling—Part 2: End-milling, International Standard, 1989. Reference number—ISO 8688-2: 1989(E).

Kwam, P., Bae, S.J., 2004. A non-linear random coefficients model for degradation testing. Technometrics 46 (4), 460–469.

Laird, N.M., Ware, J.H., 1982. Random-effects models for longitudinal data. Biometrics 38, 963–974.

Lawless, J., Hu, J., Cao, J., 1995. Methods for the estimation of failure distributions and rates from automobile warranty data. Life Time Data Anal. 1, 227–240.

Meeker, W.Q., Escobar, L.A., 1998. Statistical Methods for Reliability Data. John Wiley and Sons, New York.

Metalworking Fluids, Safety and Health Best Practices Manual, 1999.

Onar, A., Thomas, F., Choubane, B., Byron, T., 2006. Statistical mixed effects models for evaluation and prediction of accelerated pavement testing results. Transport. Eng. 132, 771–780.

Rahman, M., Kumar, A.S., Salam, M.U., 2002. Experimental evaluation on the effect of minimal quantities of lubricant in milling. Intl. J. Mach. Tools Manuf. 42, 539–547.

Sharman, A., Dewes, R.C., Aspinwall, D.K., 2001. Tool life when high speed ball nose end-milling Inconel 718. J. Mater. Process. Technol. 118 (1–3), 29–35.

Trent, E.M., 1991. Metal Cutting, third ed. Butterworth Heinmann, London.

Verbeke, G., Molenberghs, G., 1999. Linear Mixed Models on Longitudinal Data with Application to SAS.